

## The Role of Physical Processes in Determining the Interdecadal Variability of Central Arctic Sea Ice

MARIKA M. HOLLAND AND JUDITH A. CURRY

*Program in Atmospheric and Oceanic Sciences, University of Colorado, Boulder, Boulder, Colorado*

(Manuscript received 21 August 1997, in final form 20 November 1998)

### ABSTRACT

The importance of the Arctic region for global climate change has recently been highlighted in the results from general circulation model simulations under increasing atmospheric CO<sub>2</sub> scenarios. The warming that is predicted by these studies is most pronounced in the polar regions, indicating that it may be the first place in which the effects of global climate change will be detected. However, the natural variability that is present in the Arctic climate system is largely unknown and is likely to obscure the detection of anthropogenically forced changes. Additionally, there is little information on the internal processes of the Arctic ice pack, which are important for determining the variability of the ice cover.

In an effort to address these issues, the variability of the Arctic ice volume is examined using a single column sea ice–ocean mixed layer model. The model contains an ice thickness distribution and the parameterization of export and ridging due to ice divergence and shear. Variability in the ice cover is forced by applying stochastic perturbations to the air temperature and ice divergence forcing fields.

Several sensitivity tests are performed in order to assess the role of different physical processes in determining the variability of the perennial Arctic ice pack. It is found that the surface albedo and ice–ocean feedback mechanisms act to enhance the variability of the ice volume and are particularly important for the simulated response of the sea ice to fluctuations in air temperature, accounting for approximately 62% and 25% of the ice volume variance, respectively. The details of the ice thickness distribution also significantly affect the simulated variability. In particular, the ridging process acts to decrease the simulated variability of the ice pack. It reduces the variance of the ice volume by 50% when air temperature stochastic forcing is applied.

### 1. Introduction

Due to unique positive feedback mechanisms that occur at high latitudes, the extent and thickness of sea ice cover within the Arctic region are important modifiers of global climate. Decreases in sea ice extent and thickness have a large effect on the surface albedo, which allows more solar radiation to be absorbed by the earth system. This is often referred to as the surface albedo feedback. A decrease in sea ice extent and thickness also allows more efficient heat exchange between the ocean and atmosphere. These effects, which have been simulated in general circulation modeling (GCM) experiments, act to enhance the initial warming of the system. For example, in the  $2 \times \text{CO}_2$  GCM study of Manabe and Stouffer (1994), the annual average Arctic surface air temperatures warmed by approximately 9°C compared to approximately 3°C for regions in the mid-latitudes. The warming is particularly enhanced during

the winter months, when decreases in sea ice coverage strongly affect the turbulent heat exchange of the ice–ocean–atmosphere system (IPCC 1990).

Based on these results, it has been suggested (e.g., Parkinson 1992) that climate change may first be detected in the polar regions. However, the natural variability of the Arctic climate is largely unknown, in part due to the difficulties in monitoring the climate of this region. Several observational and modeling studies have examined the low-frequency variability that occurs in the Arctic system. The modeling studies to date have either employed simple one-dimensional models for simulations that span 100–1000 yr (Hakkinen and Mello 1990, hereafter HM; Bitz et al. 1996, hereafter BBMB) or full ice dynamic models for time periods of months to decades (e.g., Hibler and Walsh 1982; Walsh et al. 1985; Flato 1995). The one-dimensional modeling studies examine the model response to variability in the thermodynamic forcing, whereas dynamic modeling studies examine the effects that variability in both thermodynamic and dynamic forcing have on the simulated ice cover. From the one-dimensional model studies, it appears that natural variability in the melt season length, which occurs due to variability in the ice–atmosphere heat exchange, largely determines the variability in Arc-

---

*Corresponding author address:* Dr. Marika M. Holland, National Center for Atmospheric Research, P.O. Box 3000, Boulder, CO 80307-3000.  
E-mail: mholland@ucar.edu

tic ice volume. The dynamic sea ice models show that dynamic processes are important for accurately simulating the Northern Hemisphere sea ice variability. Within the Arctic Basin, the Beaufort Sea and the Siberian Shelf appear to exhibit the largest interannual variability in the ice cover (Flato 1995). Studies that have examined the dominant modes of variability in the observed ice extent show that the peripheral seas, in particular the Labrador and Greenland Seas, account for much of the variability in Northern Hemisphere ice extent (e.g., Slonosky et al. 1997).

This study examines the variability of an ice floe in the perennial central Arctic ice pack using a single column ice thickness distribution–ocean mixed layer model. In particular, we discuss the importance of various feedback mechanisms and ice processes for determining the natural variability of the perennial Arctic ice volume. Previous studies that employed one-dimensional models to examine these issues (HM; BBMB) did not include a full ice thickness distribution or the ridging process, although HM included ice export and open water areas within the model domain. We examine the influence that the ice thickness distribution and the processes that maintain this distribution have on the simulation of the central Arctic ice volume variability.

A single-column model cannot address mechanical feedbacks such as how changes in ice thickness will affect ice divergence. However, it does allow new insight into how the ice thickness distribution and deformation of the ice pack determine the ice volume response to variable thermodynamic and kinematic forcing. Interannual variability is forced in the model by applying realistic stochastic perturbations to the air temperature and/or ice divergence forcing. Long timescale simulations of 1000 yr are examined to determine the statistical properties, including the ice volume variance and spectral characteristics, of the simulated variability.

## 2. Model description

The model used here is a single-column ice thickness distribution model that is coupled to an ocean mixed layer model and atmospheric radiative transfer model. A detailed description of the model, including comparison with observations, can be found in Schramm et al. (1997b) and Holland et al. (1997a). This model has been used to study ice–albedo and ice–ocean feedbacks (Holland et al. 1997b), influence of snow on the ice thickness distribution (Schramm et al. 1997a), and the response of sea ice to surface heat flux perturbations (Arbetter et al. 1997).

The sea ice is modeled as an ice thickness distribution that allows for a specified number of level and ridged ice categories within the model domain. This allows us to represent the high spatial variability apparent in the observed sea ice. The different categories are described by a variety of properties including thickness, area, age, salinity, snow cover, and melt pond cover. Each category

evolves thermodynamically, independently from one another, with different interfacial heat fluxes computed for each category. New categories are created due to the freezing of open water areas and the ridging process. In order to avoid an excessive number of ice categories, a merging process occurs in which categories of similar thickness (with a preference for thick ice categories) are merged together. The thickness of the categories is not constrained in the model (as in Hibler 1980 and Flato and Hibler 1995), but instead is allowed to evolve based on the model forcing [similar to Thorndike et al. (1975) and Bjork (1992)].

In addition to thermodynamic processes, the sea ice thickness distribution is affected by mechanical forcing. Divergent sea ice motion causes sea ice to be exported from the model domain, whereas convergent motion causes ice ridging to occur. Shearing of the ice pack causes both open water and pressure ridges to form. The parameterization of these processes is done using a “redistributor” function that reorganizes the ice in the model domain based on the kinematic forcing. The redistributor used here is consistent with a plastic rheology and follows the formulation of Thorndike et al. (1975), Rothrock (1975), and Hibler (1980). Flato and Hibler (1995) have tested the sensitivity of the parameters in this redistributor in the context of an Arctic basin-scale dynamic/thermodynamic model. In the current formulation, only the thinnest 0.10 fraction of the model domain is allowed to participate in the ridging process, and it is assumed that the ridged ice is 15 times the thickness of the ice that formed the ridges (Maykut 1982). A simplified redistributor function following Bjork (1992) is used when a constant value of ice divergence is applied in the model. This function assumes a constant specified rate of open water formation due to ridging and a constant ice divergence rate. This allows ridging to occur even though convergent motion is not present in the forcing.

A complex surface albedo parameterization following Ebert and Curry (1993) is used, which considers four different spectral intervals and accounts for six different surface types including dry snow, wet snow, bare first-year ice, bare multiyear ice, melt ponds, and open water. An explicit melt pond parameterization is included in the model, whereby a specified fraction of melt water is allowed to run off the ice into the ocean, and the remainder of the water pools, into melt ponds.

The sea ice model is coupled to a bulk ocean mixed layer model (following Gaspar 1988) that has uniform temperature and salinity within the mixed layer. The mixed layer properties change due to the exchange of heat and fresh water with the atmosphere or sea ice above and the deeper ocean below. The total heat flux at the surface of the mixed layer is determined by the turbulent exchange at the ice–ocean interface, the penetration of solar radiation through ice and leads, and the fluxes (latent, sensible, and long wave) at the lead surface. The flux of freshwater at the mixed layer surface

is determined by the amount of ablation or accretion at the ice base, melt water runoff from the ice surface, brine drainage as the ice ages, freshwater inflow (representing river runoff), and precipitation and evaporation through leads. Heat and salt are also exchanged with the ocean beneath the mixed layer. This occurs through entrainment as the mixed layer deepens, and through diffusion across the mixed layer base. Frazil ice is produced when the water column becomes supercooled.

The sea ice model is also coupled to an atmospheric radiative transfer model (following Curry and Ebert 1992). Cloud characteristics and the atmospheric temperature and humidity profiles are specified externally, while the surface radiative flux is calculated spectrally using separate two-stream models for the longwave and shortwave fluxes.

Of relevance to this study, Arbetter et al. (1997) showed that this model is far less sensitive to surface heat flux perturbations than the simple one-dimensional sea ice models, which exclude ice thickness distribution and ridging effects. In a comparison to two-dimensional dynamic/thermodynamic sea ice models, the single-column model described here simulated a similar response to heat flux perturbations at the ice–ocean and ice–atmosphere interfaces.

### 3. Forcing data

To simulate the natural variability in the Arctic climate system, stochastic perturbations are applied to both the surface air temperature and ice divergence forcing fields. The stochastic perturbations are applied to a climatological annual cycle of air temperature and a constant ice divergence rate, respectively. Three standard simulations are examined with these forcings. They include 1) a simulation in which stochastic forcing is applied to the air temperature, 2) a simulation in which stochastic forcing is applied to the ice divergence field, and 3) a simulation in which stochastic forcing is applied to both the air temperature and ice divergence forcing fields. Stochastic thermodynamic forcing in a single-column model has been examined by BBMB. We expand on BBMB by examining how properties related to the ice thickness distribution and ridging processes affect the simulated variance of the ice cover. The effects of variability in the dynamic forcing of the ice cover have been studied in the context of three-dimensional models (e.g., Flato 1995). The use of a single-column model for studying the effects of variable kinematic forcing allows for relatively long simulations and numerous sensitivity tests. For all of the simulations considered here, smoothly varying climatological forcing fields are used to drive the model (Holland et al. 1997a). In cases for which stochastic forcing is not applied to the ice divergence field, a constant value of ice divergence is used. The stochastic forcing is applied as a perturbation to the relevant fields.

The stochastic perturbations are simulated using a Langevin-type equation:

$$\frac{\partial x'(t)}{\partial t} = -\frac{x'(t)}{\tau_e} + \tau_h(t)z(t), \quad (1)$$

where  $x'$  is the perturbation field that is applied to the climatological forcing;  $\tau_e$  is the characteristic timescale of the fluctuations in  $x'$ ;  $\tau_h$  is related to the variance of  $x'$ ; and  $z(t)$  represents white noise, which has zero mean and unit variance. Among other things, this stochastic model has been used to describe climate variability in sea surface temperature anomalies and sea ice anomalies (e.g., Hasselmann 1976; Reynolds 1978; Lemke et al. 1980). Following BBMB, we set  $\tau_e$  equal to five days for the thermodynamic perturbation forcing and determine  $\tau_h$  from the variance of the observed forcing field. In order to simulate a realistic time series of variability,  $\tau_h$  is obtained so that the daily variance of the stochastic forcing is approximately equal to the observed variance. In the case of the divergence forcing perturbations,  $\tau_e$  is set equal to one day and  $\tau_h$  is similarly tuned. These choices for  $\tau_e$  are consistent with the observations. The choice of  $\tau_e$  does appear to have a substantial effect on the ice volume variance. However, it does not affect the general spectral characteristics of the simulated ice–ocean system or the results from sensitivity tests. Thus, the choice of  $\tau_e$  does not appear critical for the results of this study.

Substantial interannual variability is observed in the wintertime air temperature in the Arctic, whereas the summertime air temperature remains close to the freezing point due to the relatively constant temperature of the underlying ice cover. In order to determine the variance in the observed surface air temperature, 40 yr of data from the Russian drifting ice islands were examined (NSIDC 1996). Figure 1 shows the annual cycle, daily variance, and power spectra of the surface air temperature, which is obtained from daily temperature measurements for 1954–94 for the region 75°–85°N, 160°–200°E. This data region was chosen because of its relatively consistent data coverage. The variance values have been smoothed using a 30-day running mean. The daily variance of the simulated stochastic perturbations of the air temperature field is approximately equal to these observed values.

In contrast to the surface temperature data, the ice divergence of the perennial Arctic ice pack has relatively high variance during the summer and low variance during the winter. Areas of open water are relatively small during the winter months, which impedes the ice motion and causes smaller strain rates to occur. The ice is freer to move during the summer months when thermodynamic processes cause the lead and thin ice fractions to increase. The variance of the ice divergence field was obtained from an analysis of the gridded data from the International Arctic Buoy Program. Three locations, at 78°N, 200°E; 82°N, 200°E; and 78°N, 220°E, were ex-

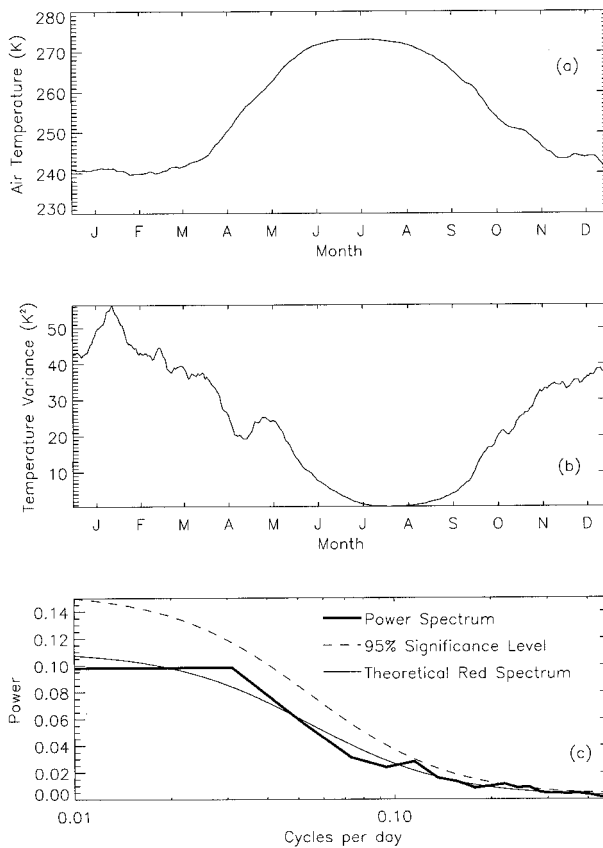


FIG. 1. The (a) average annual cycle, (b) daily variance, and (c) power spectra of daily temperature values obtained from an analysis of 40 yr of Russian ice island data. The daily variance was smoothed with a 30-day running mean.

amined for the period from 1979 to 1994. The daily variance in the divergence field from these three positions were averaged together and smoothed using a 30-day running mean to obtain the variance used in the calculation of the stochastic forcing. The annual cycle, daily variance, and power spectra of the ice divergence field from this data are shown in Fig. 2.

The spatial smoothing inherent in the gridded data buoy products will likely reduce the variance in the ice divergence field. Daily ice divergence observations from the Arctic Ice Dynamics Joint Experiment (AIDJEX) (e.g., Colony 1978) have a standard deviation of approximately  $1.7 \times 10^{-7} \text{ s}^{-1}$  over a single annual cycle. [See also Hibler et al. (1974) and Thorndike (1974) for a discussion of the AIDJEX strain rates.] For individual years from the gridded buoy data, the standard deviation is smaller, varying from  $1.0 \times 10^{-8} \text{ s}^{-1}$  to  $1.0 \times 10^{-7} \text{ s}^{-1}$ . Because the length of the AIDJEX data is approximately a year, it is impossible to examine its interannual ice divergence variability. However, it is likely that the gridded buoy data underestimate the interannual variability of the ice divergence as they do the daily variance. Thus, the stochastic forcing that is applied in this study probably is a low estimate of the actual interannual

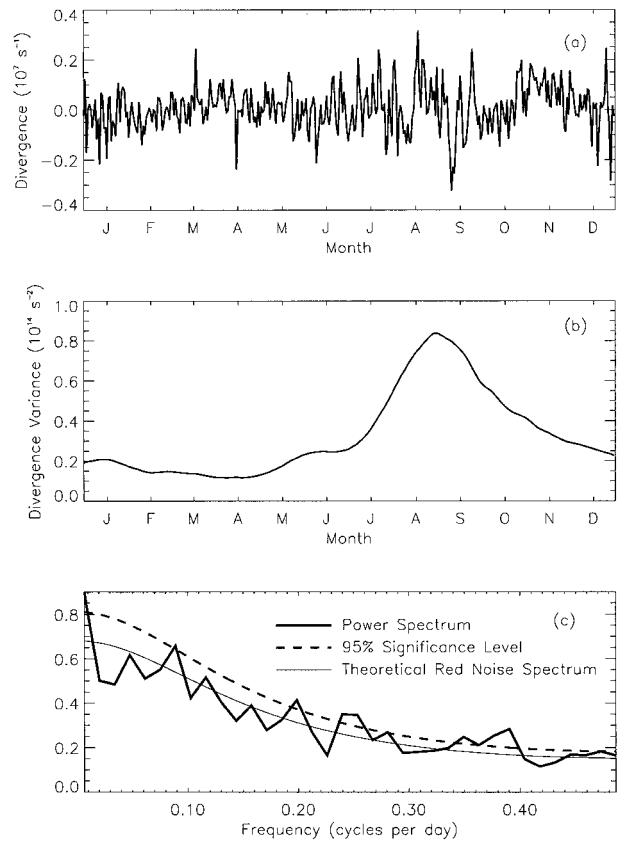


FIG. 2. The (a) average annual cycle, (b) daily variance, and (c) power spectra of the ice divergence field obtained from an analysis of gridded International Arctic Buoy Program data. The daily variance was smoothed with a 30-day running mean.

variability in the divergence of the perennial Arctic ice pack.

The divergence and shear of the ice pack are obtained from the ice velocity field:

$$\text{divergence} = \frac{\partial u}{\partial x} + \frac{\partial v}{\partial y}, \quad (2)$$

$$\text{shear} = \sqrt{\left(\frac{\partial u}{\partial x} - \frac{\partial v}{\partial y}\right)^2 + \left(\frac{\partial u}{\partial y} + \frac{\partial v}{\partial x}\right)^2}. \quad (3)$$

These are invariants of the ice deformation tensor and hence coordinate system independent. Ice divergence and shear are generally correlated. However, for simplicity it has been assumed that the stochastic forcing represents an equal perturbation to the  $\partial u/\partial x$  and  $\partial v/\partial y$  fields. This causes the shear field to remain unchanged. The effects of variable shear on the simulated variability are discussed below.

#### 4. Model response to stochastic perturbations

Three standard model simulations were performed with stochastic forcing applied to 1) the air temperature

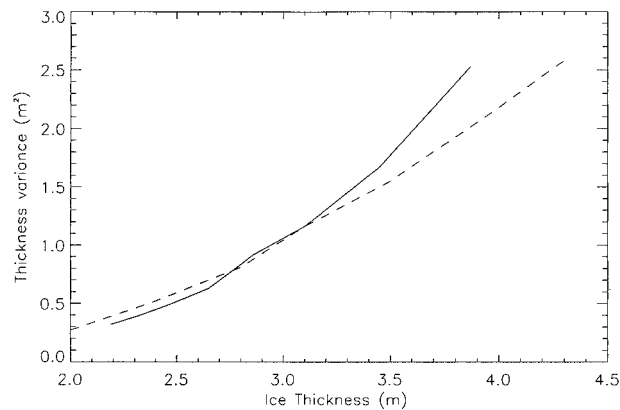


FIG. 3. The ice thickness variance as a function of mean ice thickness for cases in which the mean ice thickness is tuned using 1) longwave warming perturbations (dashed line) and 2) the mean ice divergence (solid line). Variability is forced in these simulations by applying stochastic perturbations to both the air temperature and ice divergence.

field, 2) the ice divergence field, and 3) both the air temperature and ice divergence forcing fields. Ten ice categories and a single open water category are used to represent the ice cover. The number of categories chosen for these simulations was shown to accurately represent the ice thickness distribution and ice–ocean–atmosphere exchange (Schramm et al. 1997b). The forcing used in the model simulations are based on smoothly varying climatological data (Holland et al. 1997a). The simulations were run to an equilibrium state without perturbations to the forcing and then run for an additional 1000 yr with the stochastic forcing.

Figure 3 shows the sensitivity of the ice volume variance to the mean ice thickness for cases in which the mean ice thickness is modified by changing the ice divergence or by applying a surface heat flux perturbation. As noted by BBMB, the variance increases as the mean ice thickness increases. This dependence is generally nonlinear and is different based on the model tuning. The sensitivity to the method of tuning results from changes in the ice thickness distribution and in the strength of various thermodynamic feedback mechanisms. The sensitivity of the simulated variance to these properties is discussed in sections 5 and 6. In an effort to compare the ice pack variability for different simulations without the influence of changes in the mean ice thickness, the model is tuned using the annual average value of ice divergence. This results in a mean ice thickness of 3.1 m for all of the simulations. The net ice divergence is used in this tuning because it is largely unknown. The consequences of this tuning as it relates to the sensitivity tests are discussed further in section 5.

#### Ice thickness variability

The variance of monthly ice thickness anomalies for the three standard simulations is shown in Table 1. The

TABLE 1. The variance ( $m^2$ ) of the monthly ice thickness anomalies obtained in the three standard simulations. These include cases in which stochastic forcing is applied to 1) the air temperature field, 2) the ice divergence field, and 3) both the air temperature and ice divergence fields. The variance is presented for the ice thickness and area-normalized volume of different ice types and the total area averaged ice thickness (which is equivalent to the area-normalized ice volume).

	First-year ice		Multiyear and ridged ice		Total
	Thickness	Volume	Thickness	Volume	
Case 1	0.04	0.004	0.13	0.09	0.08
Case 2	0.06	0.03	1.45	1.23	1.08
Case 3	0.07	0.03	1.56	1.31	1.16

variance is presented for different ice types and the area-averaged ice cover. The standard deviation of the average ice thickness seasonal cycle for all of the standard simulations is approximately 0.3 m. This is approximately equal to the standard deviation of monthly ice thickness anomalies in the stochastic air temperature perturbation simulation (case 1) and is less than half the standard deviation of ice anomalies obtained when stochastic forcing is applied to the ice divergence field (cases 2 and 3). Stochastic forcing of the ice divergence field appears to induce a majority of the simulated variability within the ice cover. Compared to the results from Flato (1995), the variance in the ice thickness is on the high end of what is seen in a basin-scale simulation. The differences are likely due to the longer length of the simulation in the current study (1000 vs 40 yr) and the absence of mechanical feedback mechanisms, such as the impact of ice thickness on the ice divergence.

The variability of the total ice volume is dependent on the distribution of ice types contained within the model domain. Previous one-dimensional modeling studies (e.g., HM; BBMB) did not include a full ice thickness distribution or ridging of the ice cover. Compared to these studies, the simulated ice thickness response to surface thermodynamic perturbations is relatively small. However, as is discussed in the sensitivity tests (section 5), the ridging process and an interactive ice thickness distribution act to decrease the variance of the ice pack. Thus, it is likely that the decrease in ice thickness variance compared to HM and BBMB is in part due to the inclusion within the current model of an ice thickness distribution and the processes that maintain this distribution. The impact of these processes on the simulated variability is discussed further in section 5.

Stochastic perturbations in the air temperature induce variability in the ice volume through changes in ice growth/melt. Stochastic perturbations in the ice divergence cause changes in the ice export/import within the model domain, resulting in a direct change in ice mass. In both cases, although the forcing provides power at all frequencies, the ice volume varies mainly on long timescales. This has been noted in other studies. Figure

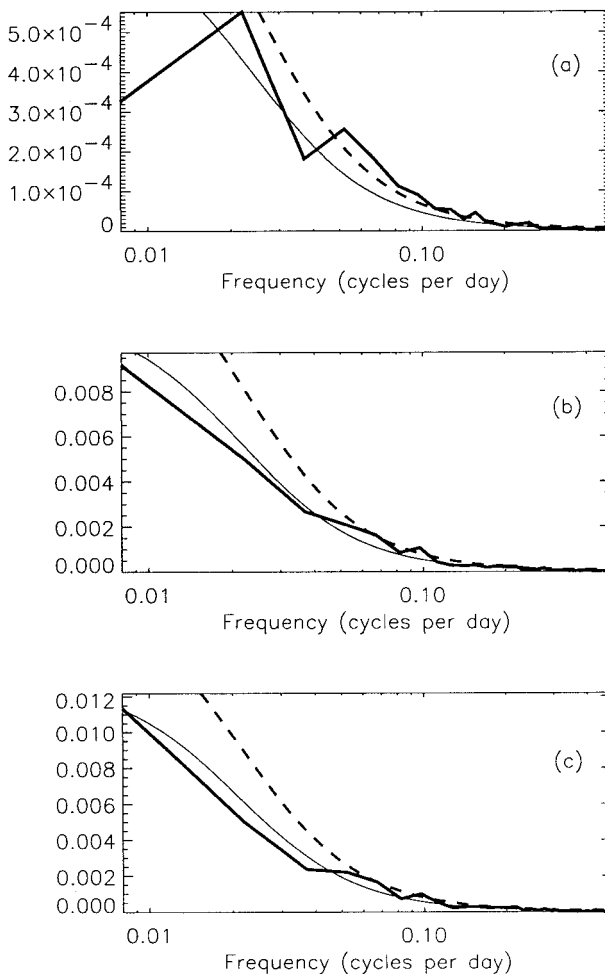


FIG. 4. The power spectrum of the annual ice thickness anomalies for (a) the air temperature stochastic forcing, (b) the ice divergence stochastic forcing, and (c) the air temperature and ice divergence stochastic forcing standard simulations. The bold line represents the spectrum, the dashed line is the 95% significance level, and the thin solid line is the theoretical red spectrum.

4 shows the power spectrum of annual ice volume anomalies for the three standard simulations. In each case, the spectra is well represented by a first-order autoregressive process (Jenkins and Watts 1968). The characteristic timescales associated with these simulations are 6.5 yr for case 1 and 7.4 yr for both cases 2 and 3.

Different ice types have different statistical properties. Thinner ice types vary on shorter timescales. In addition to the total ice volume, the volumes of different ice types are well represented by a first-order autoregressive process. This results in characteristic timescales of 0.6, 3.1, and 7.9 yr for the first-year, multiyear, and ridged ice volume, respectively. Because it more rapidly conducts heat to the ice–ocean interface, thinner ice recovers more rapidly to perturbations in surface melting caused by the variable air temperature forcing. Thin, first-year ice also has a rapid response to perturbations in the kinematic forcing due to its formation in regions

of open water and subsequent destruction during the ridging process (e.g., Flato 1995).

Hakkinen and Mellor (1990) and BBMB show that the ice thickness variability is most sensitive to perturbations in the atmospheric thermodynamic forcing at the onset of the melt season. We find that 93% of the variance in the standard air temperature stochastic forcing case is simulated when temperature perturbations are only applied during late spring and summer (1 May–31 August), and 56% of this variance is due to perturbations at the onset of the melt season (15 June–15 July). Our results are in qualitative agreement with HM and BBMB. However, compared to BBMB, a significantly larger amount of the variance in our model is due to late spring and summertime processes (93% vs 58%). This is likely due to differences in model physics between the two studies. In particular, different atmospheric models and atmosphere–ice coupling are used, with the BBMB model being perhaps freer to vary during the winter. Additionally, we speculate that the difference in model response to springtime processes is partially caused by the more sophisticated simulation of the ice–albedo and ice–ocean feedback mechanisms within the current model. These feedback mechanisms are relatively strong due to the incorporation of the ice thickness distribution and ice surface properties such as melt ponds (e.g., Curry et al. 1995). The sensitivity of the ice thickness variability to these feedback mechanisms is discussed in section 6.

In contrast to the stochastic air temperature forcing simulation, a strong seasonal signal is not seen when stochastic perturbations are applied to the ice divergence forcing for only a portion of the annual cycle. The kinematic forcing in the model consists of both divergence and shear of the ice cover. These fields share a mutual dependence on the ice velocity gradients and thus they are generally correlated. As previously mentioned, it has been assumed that the stochastic perturbations in the divergence field are caused by an equal perturbation to the  $\partial u/\partial x$  and  $\partial v/\partial y$  fields. This means that the shear of the velocity field is not affected by the stochastic perturbations to the ice divergence field. This allows us to isolate the model response to climate variability in the ice divergence/convergence. From an analysis of the International Arctic Buoy Program data, it appears that the variance present in the shear field is significantly larger than that in the divergence field. Shear is important for driving open water and ridged ice formation, and neglecting shear effects causes changes in the details of the thickness distribution. In particular, Flato and Hibler (1995) found that ridged ice volumes were changed substantially when shear effects were not included. Unlike ice divergence, shear deformation does not change the total volume of ice within the model domain, but merely redistributes it. However, due to the changes in the ice thickness distribution, the average growth rates are modified and the mean ice thickness is affected. Model simulations that apply stochastic per-

TABLE 2. The mean ice divergence values ( $\text{yr}^{-1}$ ) used in the different sensitivity studies. Three cases of forcing perturbations (pert) are shown: air temperature (tair), ice divergence (div), and both. Ocean mixed layer (OML).

	Case 1 (tair pert)	Case 2 (div pert)	Case 3 (both pert)
Standard	0.120	0.170	0.16
No OML feedbacks	0.120	0.170	0.165
No albedo feedbacks	0.130	0.175	0.17
Neither feedback	0.130	0.180	0.17
No ridging	0.070	na	na

turbations to the shear forcing (but not to the ice divergence forcing) show that the variance in the ice volume caused by stochastic perturbations in the shear field is less than  $0.01 \text{ m}^2$ . Thus, ice divergence effects largely drive the interannual variability in the ice cover for the region considered in this study.

### 5. Sensitivity to ice thickness distribution parameters

The presence of an ice thickness distribution and the processes that maintain this distribution are likely to modify the simulated variability of the ice pack relative to simple “slab” models. To elucidate the impact that these processes have on determining the climate variability of the ice cover, two sensitivity studies were performed. These include cases in which 1) the ridging process is inactive and 2) the relative fractions of first-year, multiyear, and ridged ice have been modified due to changes in the parameterization of the ridging process.

The presence of variable kinematic forcing requires that the ridging process is active. Thus, the exclusion of the ridging process (sensitivity case 1) is examined in the context of surface air temperature stochastic forcing. This simulation is compared to the standard simulation in which deformation due to ridging is induced by requiring that a certain fraction of open water is created by the ridging process (following Bjork 1992). In both simulations, a constant specified value of ice divergence causes ice export from the model domain and open water formation to occur.

As discussed by BBMB and shown in Fig. 3, the ice volume variance is a function of the mean ice thickness. As in the standard simulations, the mean ice divergence has been modified in the ridging sensitivity simulation in order to obtain the same mean ice thickness for all cases. Table 2 shows the mean ice divergence values that are used in all the simulations. The results from simulations in which no tuning has been done are also shown for comparison. In general, the results are qualitatively consistent regardless of the tuning.

The second sensitivity test in this section (sensitivity case 2) examines how changes in the relative fractions of first-year, multiyear, and ridged ice affect the simulated variability of the perennial Arctic ice cover. In the

TABLE 3. The variance ( $\text{m}^2$ ) of the monthly ice thickness anomalies obtained in sensitivity studies.

	Case 1 (tair pert)		Case 2 (div pert)		Case 3 (both pert)	
	Tuned	Un-tuned	Tuned	Un-tuned	Tuned	Un-tuned
Standard	0.08	0.08	1.08	1.08	1.16	1.16
No ridging	0.16	0.10	na	na	na	na
No OML feedbacks	0.06	0.06	0.97	0.97	1.01	1.10
No albedo feedbacks	0.03	0.04	0.91	0.98	0.96	1.13
Neither feedback	0.02	0.02	0.77	0.90	0.79	0.94

standard simulation, ridged ice is assumed to be 15 times the thickness of the ice that formed the ridges. This ridging factor and the mean ice divergence are modified in order to change the ice thickness distribution while maintaining the same area-averaged ice thickness. The sensitivity of the ice volume variance to the resulting changes in the ice thickness distribution are examined in simulations that apply stochastic forcing to both the air temperature and ice divergence forcing.

#### a. Ridging process

The effect of the ridging process on the simulated variability of the ice cover is examined by comparing the standard air temperature stochastic forcing simulation to a simulation that excludes the ridging process. Both these integrations have been forced with stochastic variability in the air temperature. They do not have variable kinematic forcing, which is only appropriate when the ridging process is active. Instead, a constant ice divergence rate is applied. As described in section 2, ridging occurs by allowing a specified fraction of open water to be created due to the ridging process. This causes ice to be redistributed in the model domain to obtain the same total ice volume but a smaller ice-covered area. The standard simulation is compared to a case in which no ridging process is active. This causes the ice thickness distribution to be maintained by the thermodynamic processes of growth and melt and by a constant specified ice divergence. This is similar to a simulation in which only an open water and single ice category are present.

The ridging process acts to dramatically decrease the variance of the area-averaged ice thickness (Table 3). This occurs even in “untuned” simulations, though the presence of ridging causes an increased ice thickness, which generally has higher variance. The spectral characteristics of the ice volume are also affected. Because the characteristic timescale is proportional to the variance, it increases when ridging is neglected from 6.5 yr for the standard simulation to 10.7 yr (7.2 yr) for the tuned (untuned) no-ridging simulation.

The ridging process causes relatively thin ice to combine into thick pressure ridges. This acts to redistribute perturbations in the thin ice into the thick end of the

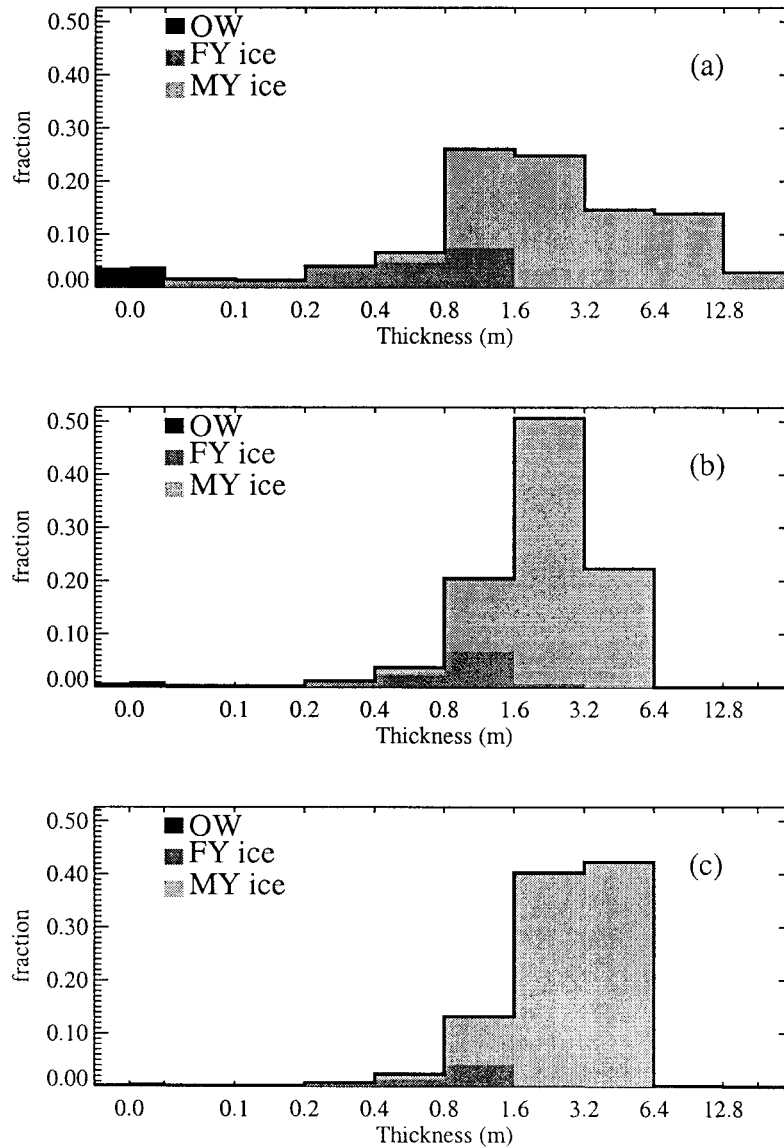


FIG. 5. The average ice thickness distribution obtained in the (a) standard simulation, (b) an untuned simulation that excludes the ridging process, and (c) a tuned simulation that excludes the ridging process. In all of these simulations, variability in the ice cover is forced by applying stochastic air temperature perturbations.

distribution. It also acts as a source of open water, a sink of relatively thin ice, and a source of relatively thick ice. Due to relatively large open water fractions, higher growth rates occur during winter. The increased open water area also allows more solar radiation into the ocean, enhancing basal melting during the summer months. The combination of these processes determines the resulting ice thickness distribution and its variability. The simulated ice thickness distribution that is obtained in these sensitivity tests is shown in Fig. 5. When ridging is excluded, the reduced open water formation causes a decrease in new ice formation and results in relatively small amounts of open water and first-year ice. The

majority of the model domain is occupied by multiyear ice from 1.6 to 6.4 m in thickness, and thick ridged ice is not present. This occurs for both tuned and untuned simulations. Although, in the tuned simulation, the multiyear ice is somewhat thicker due to the lower net ice divergence rate.

The resulting variance in the ice cover is complicated by these changes in the ice thickness distribution. The dependence of ice thickness variance on the mean ice thickness is nonlinear (Fig. 3). Ridging causes an increase in both relatively thin and thick ice. This has competing effects on the ice thickness variance, with thin ice acting to stabilize and thick ice acting to de-

TABLE 4. The values of the ridging factor and ice divergence ( $\text{yr}^{-1}$ ) used in a sensitivity study that examines the impact of the ice thickness distribution on the simulated ice thickness variance.

Ridging factor	2	3	5	10	15	20	25
Mean divergence	0.115	0.125	0.135	0.150	0.160	0.170	0.175

stabilize the ice pack. The thin ice effects dominate in determining the basal accretion rates, causing a higher area-averaged ice growth rate when ridging is included. It appears that changes in the area-averaged ice thickness variance are also consistent with changes in the thin ice area. Thus, the stabilizing impact of the ridging process is likely due to changes in the ice mass balance, which are affected (and dominated) by changes in the thin ice area.

Clearly, the simulated variability of the ice cover is a function of mean ice thickness *and* the ice thickness distribution. The inclusion of the ridging process is important for both open water and thick ice formation. This affects the simulated ice thickness distribution and, in turn, the simulated climate variability of the ice cover.

### b. Representation of the ice thickness distribution

The ice thickness distribution is maintained by a variety of processes including ice deformation, ice export, and the thermodynamic processes of growth and melt. Depending on the parameterization of these processes, many different ice thickness distributions can result with the same mean thickness. As discussed in the ridging sensitivity test, the details of the ice thickness distribution appear to play an important role in determining the variability of the ice pack. This section examines the ice volume variance that occurs for different realizations of the ice thickness distribution. Although the relative fractions of first-year, multiyear, and ridged ice are different for the simulations examined here, they all maintain the same mean ice thickness of approximately 3.1 m. Different ice thickness distributions are obtained by changing the factor that determines the thickness of ridged ice. In the standard simulation, ridged ice is assumed to be 15 times the thickness of the ice that formed the ridges. This ridging factor and the mean ice divergence rate are modified to obtain different ice thickness distributions that have the same mean ice thickness. These simulations are forced with stochastic perturbations applied to both the air temperature and ice divergence.

Table 4 shows the ridging factor and the corresponding ice divergence rate that are used in these studies. As the ridging factor increases, thicker ridged ice that occupies a smaller area is created. This causes more open water formation and an increase in new ice growth. The presence of more thin ice and open water area increases the ice growth rates and results in thicker mean ice. In order to compensate for these effects and maintain an ice thickness of 3.1 m, a higher ice divergence rate is used. The resulting impact of increasing both the ridging factor and ice export is that the first-year ice area, thickness, and volume increase (Fig. 6). At the same time, the multiyear and ridged ice thicknesses increase, while their area and volume decrease. The average basal accretion and ablation rates also increase with the increasing ridging factor due to the larger thin ice areas.

These modifications of the ridging process and the resulting changes in the ice thickness distribution cause changes in the simulated ice thickness variance. Figure 7 shows the ice thickness variance as a function of the first-year ice area for these simulations. As the thin ice area increases, the area-averaged ice thickness variance decreases. This is consistent with the results from the ridging sensitivity study. Both the details of the subgrid-scale ice thickness distribution and the processes that

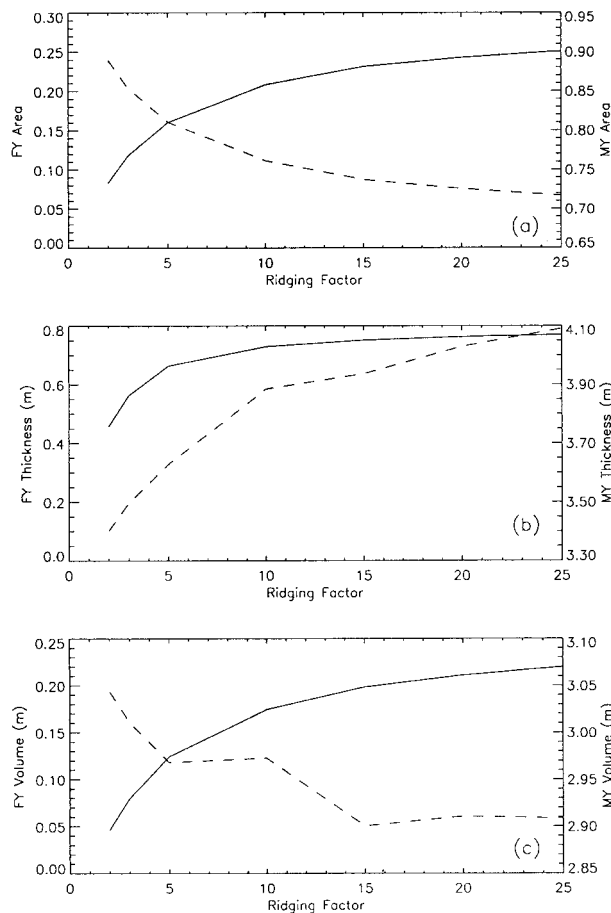


FIG. 6. The (a) fractional ice area, (b) ice thickness, and (c) area-weighted ice volume for first-year (solid) and multiyear (dashed) ice obtained as a function of the ridging factor. The left axis shows the first-year (FY) ice values and the right axis shows the multiyear (MY) ice values.

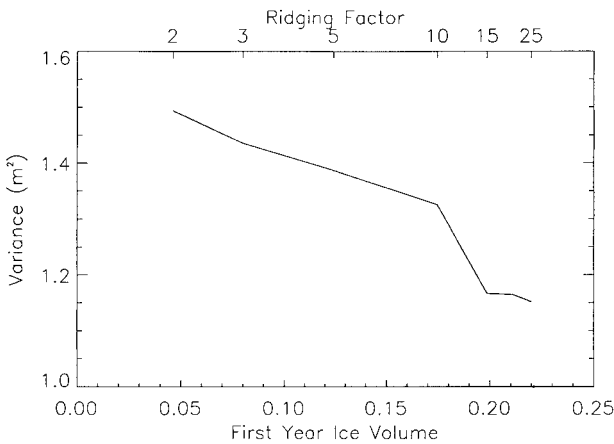


FIG. 7. The variance of the total area-averaged ice thickness as a function of the first-year ice volume (bottom scale) and the ridging factor (top scale). These results are obtained in simulations that maintain the same mean ice thickness while obtaining different representations of the ice thickness distribution.

maintain this distribution are important factors for determining the variability of the ice cover. For this study, it appears that a decrease in ice thickness variance is consistent with an increase in thin first-year ice area.

## 6. Sensitivity to ice–albedo and ice–ocean feedback mechanisms

The albedo and ocean feedback mechanisms that are present in this model have been discussed in Holland et al. (1997b). A surface warming perturbation will result in changes within the perennial ice pack. These include a decrease in the duration of the snow cover, a decrease in the thickness of the ice, an increase in the amount of open water that occurs within the pack ice, and changes in the surface melt pond characteristics. The changes that occur in these properties act to decrease the surface albedo, allowing more shortwave radiation to be absorbed by the ice–ocean system. This positive albedo feedback mechanism reinforces the sea ice response to the initial warming perturbation.

The primary ocean feedback that is present in the model also enhances initial perturbations of the ice–ocean system. An initial increase in open water area or decrease in ice thickness will allow more solar radiation to be absorbed in the ocean mixed layer. This increases the mixed layer heat content and results in larger ice–ocean interfacial heat fluxes. A further decrease in ice thickness and increase in open water area results. In Holland et al. (1997b), it was shown that the albedo and ocean feedback mechanisms are not generally independent.

It should be noted that ice dynamic feedbacks, which are not included in this model, would likely play an important role in the sensitivity of the perennial ice pack to these thermodynamic feedback mechanisms. Thermodynamically induced changes in the ice mass balance

will, in turn, cause changes in the ice motion (and further changes in the ice mass balance). This model cannot address these issues and instead will examine these thermodynamic feedback mechanisms in the absence of any dynamic feedbacks that would occur in the real climate system.

The sensitivity to the ice–albedo and ice–ocean feedback mechanisms is examined by comparing the standard simulations discussed in section 4 to cases in which these feedback mechanisms are inactive. The ice–albedo feedback is excluded by forcing the area-averaged surface albedo to remain at the annual cycle of equilibrium values that are obtained in the standard simulations. Similarly, ocean feedback processes are excluded by forcing the annual cycle of ocean mixed layer temperature, salinity, and depth to remain at the equilibrium values. Table 3 shows the monthly ice thickness variance obtained in these sensitivity studies.

When the ice–albedo and ice–ocean feedback mechanisms are inactive, the variance of the monthly ice thickness is reduced compared to the corresponding standard simulation for all cases of stochastic forcing. Both feedbacks act to enhance perturbations of the ice–ocean system, which increases the variability in the simulated ice cover. The ice–albedo and ice–ocean feedback mechanisms are particularly important for the climate variability simulated when stochastic perturbations are applied to the air temperature forcing. In this case, they account for approximately 62% and 25% of the standard simulation ice thickness variance, respectively (Table 3). The combined effects of the surface albedo and ocean mixed layer feedbacks account for approximately 75% of the ice thickness variance in the standard air temperature stochastic forcing simulation.

When stochastic forcing is applied to the ice divergence field, the ice–albedo and ice–ocean feedback mechanisms account for only about 15% and 10%, respectively, of the area-averaged ice thickness variance present in the corresponding standard simulation. High-frequency variations in the ice divergence field cause changes in the rate of open water formation, which will affect the surface albedo and penetration of solar radiation into the ocean mixed layer. This, in turn, will affect the ice–albedo and ice–ocean feedback mechanisms. However, the direct effect of stochastic variability in the ice divergence field induces variability in the ice deformation and the transport of ice into or out of the model domain. This has a significantly large effect on the simulated mass balance of the ice cover and reduces the importance of the ice–albedo and ice–ocean feedback mechanisms for determining the ice thickness variance.

The ice–albedo and ice–ocean feedback mechanisms account for approximately 17% and 13% of the corresponding standard simulation ice thickness variance, respectively, when stochastic perturbations are applied to both the air temperature and the ice divergence forcing. Compared to the ice divergence stochastic forcing sim-

ulation, the air temperature perturbations excite these feedback mechanisms and enhance the variability of the ice cover.

## 7. Discussion and conclusions

The response of a single cell ice thickness distribution–ocean mixed layer model to simulated climate variability has been examined. The general statistical properties of the simulated variability are similar to what has been obtained in previous studies (e.g., Hakkinen and Mellor 1990; Flato 1995; Bitz et al. 1996). In particular, the ice volume varies predominantly on interdecadal timescales, and the ice thickness variability is particularly sensitive to fluctuations in air temperature at the onset of the melt season.

Stochastic perturbations in the ice divergence result in a variance of  $1.08 \text{ m}^2$  in the monthly area-averaged ice thickness. Air temperature forcing stochastic perturbations cause a much lower variance in the ice cover (of  $0.08 \text{ m}^2$ ). Compared to Bitz et al. (1996), Battisti et al. (1997), and Hakkinen and Mellor (1990), a significantly smaller variance in the ice thickness is induced by stochastic fluctuations of the thermodynamic forcing. It appears likely that this is due, in part, to the inclusion of an ice thickness distribution and the ridging process within the current model. This hypothesis is consistent with the results from sensitivity tests that examine the model response to the ridging process. When ridging is neglected, the variance of the ice cover is approximately double that of the standard simulation.

The ice–albedo and ice–ocean feedback mechanisms have a large impact on the model response to stochastic perturbations in the air temperature, accounting for approximately 62% and 25% of the ice volume variance, respectively. The combined albedo and ocean feedback mechanisms account for approximately 75% of the ice volume variance when stochastic air temperature forcing is applied. This impact is reduced but still important in simulations that apply stochastic perturbations to the ice divergence field. For example, when stochastic perturbations are applied to both the air temperature and ice divergence fields, the combined albedo and ocean feedbacks account for 32% of the ice volume variance. The presence of an ice thickness distribution that allows for a more accurate simulation of the penetration of solar radiation within the ice and ocean and the inclusion of surface properties that affect the albedo, such as the formation and evolution of melt ponds, are important for the accurate simulation of ocean and albedo feedback mechanisms (e.g., Curry et al. 1995; Holland et al. 1997a). Thus, the inclusion of these processes is suggested for future modeling efforts that examine the natural variability of the Arctic ice cover.

The details of the ice thickness distribution are also very important for accurately simulating the variability of the Arctic ice pack. As discussed by BBMB, the variance in the ice thickness anomalies is dependent on

the ice thickness. This relationship is nonlinear. Thus, although the area-averaged ice thickness may remain constant, differences in the relative area and thickness of different ice types will result in different simulations of sea ice variability. It appears that changes in the thin end of the distribution are particularly important for simulating the variability of the ice volume. In the simulations considered here, the variance and correlation timescale of the ice volume generally increased when the area of thin first-year ice was reduced due to modifications of the ridging process.

The advection of the ice cover, the ridging process, and the resolution of the ice thickness distribution all act to modify the simulated ice thickness distribution and are important components of accurately modeling the low-frequency variability of the ice cover. In particular, as shown by this study, the ridging process acts to reduce the natural variability of the ice pack, causing up to a 50% decrease in the ice volume variance. It also causes changes in the spectral characteristics of the ice volume, resulting in shorter correlation timescales when ridging is active.

The results obtained here are from a single-column model, and the impact of these processes in three-dimensional and fully coupled model simulations should also be examined. However, it appears likely that the subgrid-scale parameterizations of the ridging process and the ice thickness distribution will play an important role in improving simulations of Arctic variability.

*Acknowledgments.* We would like to thank Dr. C. M. Bitz and two anonymous reviewers for helpful comments on this paper. This research was supported by NSF OPP-9614492.

## REFERENCES

- Arbeter, T. E., J. A. Curry, M. M. Holland, and J. A. Maslanik, 1997: Response of sea ice models to perturbations in surface heat flux. *Ann. Glaciol.*, **25**, 193–197.
- Battisti, D. S., C. M. Bitz, and R. E. Moritz, 1997: Do general circulation models underestimate the natural variability in the Arctic climate? *J. Climate*, **10**, 1909–1920.
- Bitz, C. M., D. S. Battisti, R. E. Moritz, and J. A. Beesley, 1996: Low-frequency variability in the Arctic atmosphere, sea-ice, and upper-ocean climate system. *J. Climate*, **9**, 394–408.
- Bjork, G., 1992: On the response of the equilibrium thickness distribution of sea ice to ice export, mechanical deformation, and thermal forcing with application to the Arctic Ocean. *J. Geophys. Res.*, **97**, 11 287–11 298.
- Colony, R., 1978: Daily rate of strain of the AIDJEX manned triangle. *AIDJEX Bull.*, **39**, 85–110.
- Curry, J. A., and E. E. Ebert, 1992: Annual cycle of radiation fluxes over the Arctic Ocean: Sensitivity to cloud optical properties. *J. Climate*, **5**, 1267–1280.
- , J. L. Schramm, and E. E. Ebert, 1995: Sea ice–albedo climate feedback mechanism. *J. Climate*, **8**, 240–247.
- Ebert, E. E., and J. A. Curry, 1993: An intermediate one-dimensional thermodynamic sea ice model for investigating ice–atmosphere interactions. *J. Geophys. Res.*, **98**, 10 085–10 109.
- Flato, G. M., 1995: Spatial and temporal variability of Arctic ice thickness. *Ann. Glaciol.*, **21**, 323–329.

- , and W. D. Hibler III, 1995: Ridging and strength in modeling the thickness distribution of Arctic sea ice. *J. Geophys. Res.*, **100**, 18 611–18 626.
- Gaspar, P., 1988: Modeling the seasonal cycle of the upper ocean. *J. Phys. Oceanogr.*, **18**, 161–180.
- Hakkinen, S., and G. L. Mellor, 1990: One hundred years of Arctic ice cover variations as simulated by a one-dimensional, ice-ocean model. *J. Geophys. Res.*, **95**, 15 959–15 969.
- Hasselmann, K., 1976: Stochastic climate models, Part I. Theory. *Tellus*, **28**, 473–485.
- Hibler, W. D., III, 1980: Modeling a variable thickness sea ice cover. *Mon. Wea. Rev.*, **108**, 1943–1973.
- , and J. E. Walsh, 1982: On modeling seasonal and interannual fluctuations of Arctic sea ice. *J. Phys. Oceanogr.*, **12**, 1514–1523.
- , W. F. Weeks, A. Kovacs, and S. F. Ackley, 1974: Differential sea-ice drift. I. Spatial and temporal variations in sea-ice deformation. *J. Glaciol.*, **13**, 437–455.
- Holland, M. M., J. A. Curry, and J. L. Schramm, 1997a: Modeling the thermodynamics of a sea ice thickness distribution. 2. Sea ice/ocean interactions. *J. Geophys. Res.*, **102**, 23 093–23 107.
- , J. L. Schramm, and J. A. Curry, 1997b: Thermodynamic feedback processes in a single-column sea ice/ocean model. *Ann. Glaciol.*, **25**, 327–332.
- IPCC, 1990: *Climate Change: The IPCC Scientific Assessment*. Cambridge University Press, 365 pp.
- Jenkins, G. M., and D. G. Watts, 1968: *Spectral Analysis and Its Applications*. Holden-Day, 525 pp.
- Lemke, P., E. W. Trinkl, and K. Hasselmann, 1980: Stochastic dynamic analysis of polar sea ice variability. *J. Phys. Oceanogr.*, **10**, 2100–2120.
- Manabe, S., and R. J. Stouffer, 1994: Multiple-century response of a coupled ocean–atmosphere model to an increase of atmospheric carbon dioxide. *J. Climate*, **7**, 5–23.
- Maykut, G. A., 1982: Large-scale heat exchange and ice production in the central Arctic. *J. Geophys. Res.*, **87**, 7971–7984.
- NSIDC, 1996: *Arctic Ocean Snow and Meteorological Observations from Drifting Stations, 1937, 1950–1991*, Version 1.0, NSIDC, CD-ROM.
- Parkinson, C. L., 1992: Spatial patterns of increases and decreases in the length of the sea ice season in the North Polar region, 1979–1986. *J. Geophys. Res.*, **97** (C9), 14 377–14 388.
- Reynolds, R. W., 1978: Sea-surface temperature anomalies in the North-Pacific Ocean. *Tellus*, **30**, 97–103.
- Rothrock, D. A., 1975: The energetics of the plastic deformation of pack ice by ridging. *J. Geophys. Res.*, **80** (33), 4514–4519.
- Schramm, J. L., M. M. Holland, and J. A. Curry, 1997a: The effects of snowfall on a snow-ice-thickness distribution. *Ann. Glaciol.*, **25**, 287–291.
- , —, —, and E. E. Ebert, 1997b: Modeling the thermodynamics of a sea ice thickness distribution. Part 1: Sensitivity to ice thickness resolution. *J. Geophys. Res.*, **102**, 23 079–23 091.
- Slonosky, V. C., L. A. Mysak, and J. Derome, 1997: Linking Arctic sea-ice and atmospheric circulation anomalies on interannual and decadal timescales. *Atmos.–Ocean*, **35**, 333–366.
- Thorndike, A. S., 1974: Strain calculations using AIDJEX 1972 position data. *AIDJEX Bull.*, **24**, 107–129.
- , D. A. Rothrock, G. A. Maykut, and R. Colony, 1975: The thickness distribution of sea ice. *J. Geophys. Res.*, **80**, 4501–4513.
- Walsh, J. E., W. D. Hibler III, and B. Ross, 1985: Numerical simulation of Northern Hemisphere sea ice variability, 1951–1980. *J. Geophys. Res.*, **90**, 4847–4865.